

## Synthesis and Characterization of $\text{CuNb}_2\text{O}_6$ from an Oxalic Precursor Via Solid State Reaction

Maria Veronilda Macedo Souto<sup>a,\*</sup>, Maria José Santos Lima<sup>a</sup>, Cleonilson Mafra Barbosa<sup>a</sup>, Uilame Umbelino Gomes<sup>b</sup>, Carlson Pereira de Souza<sup>c</sup>, Camila Pacelly Brandão de Araújo<sup>c</sup>

<sup>a</sup>Universidade Federal do Rio Grande do Norte – UFRN, Tecnologia, Departamento de Ciência e Engenharia de Materiais, Natal, RN, Brazil

<sup>b</sup>Universidade Federal do Rio Grande do Norte – UFRN, Centro de Ciências Exatas, Departamento de Física Teórica e Experimental, Natal, RN, Brazil

<sup>c</sup>Universidade Federal do Rio Grande do Norte – UFRN, Tecnologia, Departamento de Engenharia Química, Natal, RN, Brazil

Received: January 17, 2016; Accepted: June 13, 2016

The present paper's objective was to synthesize and characterize both the oxalic niobium precursor  $(\text{NH}_4)_3\text{NbO}(\text{C}_2\text{O}_4)_3 \cdot \text{H}_2\text{O}$ , and the product of its doping with Cu and calcining,  $\text{CuNb}_2\text{O}_6$ . In order to obtain the niobium precursor, commercially available niobium oxide ( $\text{Nb}_2\text{O}_5$ ) was subject to fusion with potassium bisulfate ( $\text{KHSO}_4$ ). Once leached with water, the powder was complexed with oxalic acid and ammonium oxalate. The as produced material was manually mixed with copper nitrate  $\text{Cu}(\text{NO}_3)_2 \cdot 2\text{H}_2\text{O}$  (25% Cu molar) and calcined at  $1000^\circ\text{C}$  in a muffle furnace.  $\text{CuNb}_2\text{O}_6$  was then obtained. The precursor was characterized by XRD, SEM, FT-IR, XRF, TG/DTG. The calcination product was characterized by XRD, XRF and SEM. Results show that single phase  $\text{CuNb}_2\text{O}_6$  could be obtained by this method without  $\text{Nb}_2\text{O}_5$  contamination.

**Keywords:** Precursor, solid-solid reaction, niobium oxide, copper, doping

### 1. Introduction

The use of niobium containing materials' has gained much attention, on the later decades, due its various industrial applications. Among these, particular emphasis has been given to its use by aerospace industry, on the production of special alloys, as well as by electro-electronic industry, where those materials find application as capacitors Lima, 2010<sup>1</sup>; Critical raw materials, 2013<sup>2</sup>.

According to Lopes et.al 2014<sup>3</sup>, the use of those materials on several different industrial sectors has been making niobium a decisive element on for the worldwide industrial development. For Brazil, the large scale use of niobium materials is of utmost importance as it possesses over 90% of the world's niobium reserves Leite, 1988<sup>4</sup>.

Another use for niobium based materials that has grown in importance is in heterogeneous catalysis, where those materials have presented higher catalytic activity, selectivity and chemical stability than traditional noble metal based catalysts (Tanabe, 1990<sup>5</sup>, specially niobium oxides. Investigation on niobium oxides has focused on new active phases, promoters Ziolk, 20036 or supports Oliveira et. al, 2007<sup>7</sup>; Cardoso et. al, 2012<sup>8</sup>.

Main niobium oxides are: niobium pentoxide ( $\text{Nb}_2\text{O}_5$ ), niobium dioxide ( $\text{NbO}_2$ ) and niobium oxide ( $\text{NbO}$ ). Among these, the first is the most stable Lee, 1999<sup>9</sup>.

On this paper, commercially available niobium pentoxide ( $\text{Nb}_2\text{O}_5$ ) was used as a starting material for the synthesis of the precursor  $(\text{NH}_4)_3\text{NbO}(\text{C}_2\text{O}_4)_3 \cdot \text{H}_2\text{O}$  (trioxalate monohydrated ammonium oxiniobate), which was used for the production of niobium- copper mixed oxide.

According to Mathern and Rohmer 1969<sup>10</sup> this precursor presents three oxalic groups in coordination with the metal-oxygen  $\text{Nb}=\text{O}$  core and forms a coordination compound with 5 bonds in the form of a coordination polyhedron with a pentagonal bi-pyramid structure with the given chemical formula.

This precursor's use for the synthesis of niobium oxides has been proved feasible and interesting as it presents higher reactivity than the commercial niobium pentoxide, which allows the production of mixed oxides in single phases, without the presence of a second niobium oxide phase ( $\text{Nb}_2\text{O}_5$  usually). This is due to its shape and small particle sizes ( $<2\mu\text{m}$ ). Medeiros, 2002<sup>11</sup> was able to decrease both time and temperature require for the synthesis of niobium carbide via gas solid reaction by using this material as niobium source. Traditional processes required temperatures over  $1400^\circ\text{C}$  with long reaction times ( $>6\text{h}$ ) whilst this method was able to produce NbC at temperatures in the range from  $820 - 980^\circ\text{C}$  with 60-120min soaking time. Oliveira 2014<sup>12</sup> used this precursor for the synthesis of  $\text{Nb}_2\text{O}_5$  and compared its catalytic activity to commercially available niobium pentoxide for the oleic acid esterification reaction, and owed to the precursor the higher yield achieved.

Such characteristics justify the use of this precursor for the synthesis of niobium and copper mixed oxide in this paper.

Copper was chosen as the second metal of the oxide phase as it is known to enhance catalytic activity in hydrogen oxidation processes'. Furthermore,  $\text{Cu}^{2+}$  ions can modify magnetic behavior and electric transportation mechanism of the oxide Vasconcelos, 2010<sup>13</sup> which can be interesting for use in capacitors or electrochemical reactions' catalysts.

\* e-mail: [veronilda.macedo@gmail.com](mailto:veronilda.macedo@gmail.com)

In face of the characteristics and applications here exposed, as well as the need of developing new routes for the processing of niobium in Brazil, this paper aims to produce niobium and copper mixed oxide,  $\text{CuNb}_2\text{O}_6$  by solid state reaction of the precursor  $[(\text{NH}_4)_3\text{NbO}(\text{C}_2\text{O}_4)_3 \cdot n\text{H}_2\text{O}]$  with copper nitrate, and characterize these materials.

## 2. Methodology

On this paper, refractory metals' oxides were produced by solid state reaction in a muffle furnace using fine  $(\text{NH}_4)_3\text{NbO}(\text{C}_2\text{O}_4)_3 \cdot \text{H}_2\text{O}$  precursor as starting material.

For the precursor's synthesis, commercially available niobium oxide ( $\text{Nb}_2\text{O}_5$ , Sigma Aldrich, 94.55%) was fused in platinum crucible with potassium bisulfate ( $\text{KHSO}_4$ , Sigma Aldrich, 96.55%) at 1:7 wt. ratio. Afterwards it was crushed and decanted in water for 12h. Then, the solid was leached with hot water and later stirred with oxalic acid ( $\text{H}_2\text{C}_2\text{O}_4$ , Sigma Aldrich, 99.95%) and ammonium oxalate ( $\text{C}_2\text{H}_8\text{N}_2\text{O}_4$ , Sigma Aldrich, 99.99%) at a 1:3 wt. ratio. The as produced material was then slowly evaporated with continuous stirring at  $60^\circ\text{C}$  to promote particles agglomeration, and dried in muffle furnace for 24h. This process is in accordance to the methodology proposed by Medeiros. This powder was characterized by TG/DTG (SDT-600 TA instruments,  $\text{N}_2$  atmosphere), FT-IR (Spectrophotometer Perkin Elmer – 16PC) and SEM (SHIMADZU MEV SSX550) in order to better understand it weight loss behavior, morphology and chemical bonds, which could affect the mixed oxide derived from it.

For the production of the mixed Nb/Cu oxide Vasconcelos' 2010<sup>13</sup> methodology was used, this method consists on manually mixing the as produced precursor with copper nitrate ( $\text{Cu}(\text{NO}_3)_2$ , Sigma Aldrich, 99.99%) in stoichiometric amounts according to the ratio Cu/Nb desired with the help of mortar and pestle. In this issue Cu/Nb= 25% molar.

The mixed powder was placed on a ceramic crucible and loaded to a muffle furnace (EDG Inox Line 3000, Brazil). The furnace was heated with a  $5^\circ\text{C} \cdot \text{min}^{-1}$  heating rate from room temperature ( $25^\circ\text{C}$ ) to  $980^\circ\text{C}$  and held for 180min. The soaking time was established so that single phase  $\text{CuNb}_2\text{O}_6$  could be obtained.

The as produced powder was characterized by XRF (SHIMADZU EDX-720, air atmosphere), SEM (SHIMADZU MEV SSX550), XRD (SHIMADZU XRD- 6000, Cu-K $\alpha$ , at 30 kV and 30 mA, with  $2^\circ \cdot \text{min}^{-1}$  step).

## 3. Results and Discussion

### 3.1 Precursor's characterization

The precursor was characterized by thermogravimetric analysis (TG), as well as infra-red spectroscopy (IR) and scanning electron microscopy (SEM).

#### 3.1.1 Infra-Red Spectroscopy

Figure 1 presents the IR spectra of the oxalic precursor. The binding bands close to  $3539 \text{ cm}^{-1}$  occur due to presence of ammonia molecules in the precursor. The bands on the region

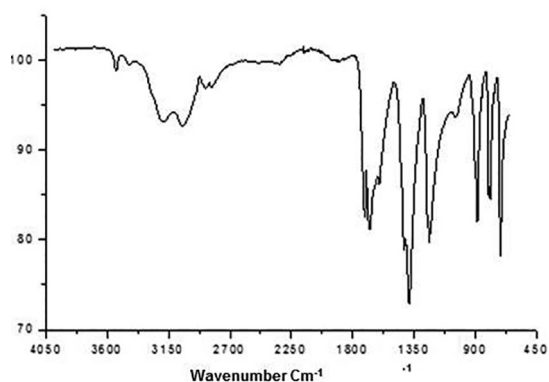


**Figure 1:** IR spectra of the niobium precursor  $(\text{NH}_4)_3\text{NbO}(\text{C}_2\text{O}_4)_3 \cdot \text{H}_2\text{O}$ .

of  $3442 \text{ cm}^{-1}$  and  $3212 \text{ cm}^{-1}$  are related to the crystallization water. Those between  $1714 \text{ cm}^{-1}$  and  $1241 \text{ cm}^{-1}$  refer to oxalic and oxalate groups in coordination with Nb, as well as the band at  $793 \text{ cm}^{-1}$  which can also be attributed to those groups. It can be noted bands occurring at  $889 \text{ cm}^{-1}$ , which refer to the Nb=O bond, according to Marta et. Al, 1983<sup>14</sup>.

#### 3.1.2 TG/DTG analysis

Thermal stability of the precursor was evaluated by exploratory TG/DTG analysis carried out in nitrogen atmosphere with  $5^\circ\text{C} \cdot \text{min}^{-1}$  heating rate from room temperature to  $1000^\circ\text{C}$

Figure 2 and Table 1 present the mass loss profile and the temperature ranges for each of the six steps identified. The first two steps occur in the range from  $25^\circ\text{C}$  to  $128^\circ\text{C}$  and correspond to a dehydration /crystallization process accounting for 6.02 % mass loss (0.43157mg). From  $128^\circ\text{C}$  to  $593^\circ\text{C}$  four other weight loss events take place, and account for 73.73 % (4.3493mg). Third and fourth events, occurring in the range from  $128^\circ\text{C}$  and  $306^\circ\text{C}$ , correspond to the decomposition of the ammonium oxalate part of the structure, with the liberation of  $\text{CO}$ ,  $\text{CO}_2$  and  $\text{NH}_3$ . From  $306^\circ\text{C}$  to  $593^\circ\text{C}$  two other mass loss' events take place, accounting for 10.54% weight loss (1.8733mg). These could be attributed to the  $\text{CO}_2$  evolution or to the crystallization of the decomposed material. However this event is not attributed to a decomposition step of the niobium complex, according to Marta et. al 1983<sup>14</sup>, and was, therefore, signed to the desorption of the gas, which was produced at low temperature and was adsorbed on the complex' surface. Further on, no other weight loss event can be noted and one can say that all volatile matter was eliminated. Therefore, the decomposition study from TG-DTG analysis accounted for a total 73.73% weight loss.

#### 3.1.3 XRD analysis

Figure 3 presents the XRD profile for the oxalic niobium precursor  $(\text{NH}_4)_3\text{NbO}(\text{C}_2\text{O}_4)_3 \cdot \text{H}_2\text{O}$ . The XRD pattern presents high intensity peaks (the most intense at  $29.70^\circ$ ), characteristic of crystalline materials, while presenting also an amorphous part, responsible for the interference on the produced pattern, according to Lu 2001<sup>15</sup>.

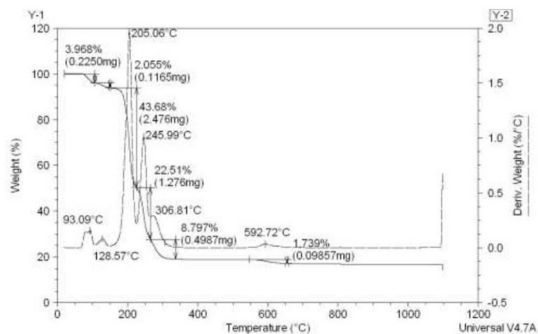


**Figure 2:** TG/DTG profile for the niobium precursor.

**Table 1:** Thermogravimetric evaluation of the  $(\text{NH}_4)_3[\text{NbO}(\text{C}_2\text{O}_4)_3] \cdot \text{H}_2\text{O}$  from room temperature to 1000°C.

Material	Steps	$T_i$ (°C)	$T_f$ (°C)	Weight (%)
$(\text{NH}_4)_3[\text{NbO}(\text{C}_2\text{O}_4)_3] \cdot \text{H}_2\text{O}$	1	25	94	3.97
	2	94	128	2.05
	3	128	205	43.68
	4	205	307	22.51
	5	306	320	8.79
	6	320	593	1.74

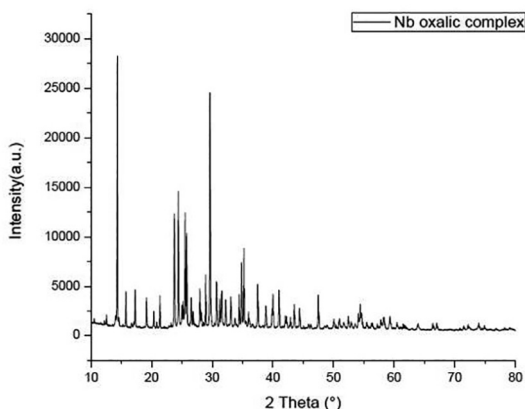


**Figure 3:** XRD pattern of the niobium complex  $[(\text{NH}_4)_3\text{NbO}(\text{C}_2\text{O}_4)_3 \cdot n\text{H}_2\text{O}]$ .

### 3.1.4. SEM analysis

Figures 4(a) and (b) present the morphology of the oxalic precursor through SEM analysis of the material with 1000x and 5000x amplifications. Circled region of Figure 4(a) highlight small particles' agglomerates. Amorphous regions can be observed as well, which is in agreement with the XRD pattern for this material. On Figure 4(b) larger particles can be observed.

Particles of different shapes are present in the agglomerate displayed in Figure 4a, some of which have spherical form, while others are the form of platelets. According to Medeiros, 2002<sup>11</sup>, these aspects depend on how the complex powder is obtained from the complexing solution, i.e. on evaporation parameters, which can produce various materials in terms of particle shape and agglomerate sizes, though chemical characteristics are the same regardless of them.

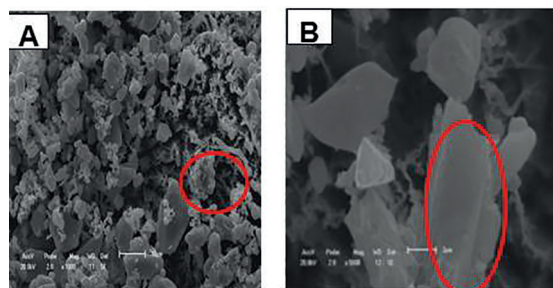


**Figure 4:** SEM image of the niobium complex (precursor), (a) 1000x and (b)5000x.

## 3.2. Characterization of niobium and copper mixed oxide

Niobium and copper mixed oxide was synthesized with 25% Cu (molar) and characterized by XRD, SEM-EDS and XRF.

### 3.2.1 XRD analysis and Rietveld refinement with Maud software

Niobium and copper mixed oxide,  $\text{CuNb}_2\text{O}_6$ , (ICSD 71606- orthorhombic) was synthesized with 25% molar Cu and its XRD pattern is presented on Figure 5. Intense and characteristic peaks, mainly at  $\theta=31.62^\circ$ , can be easily identified. This compound was also identified by other authors (Vasconcelos, 2010<sup>13</sup>) however  $\text{Nb}_2\text{O}_5$  was also present in those papers.

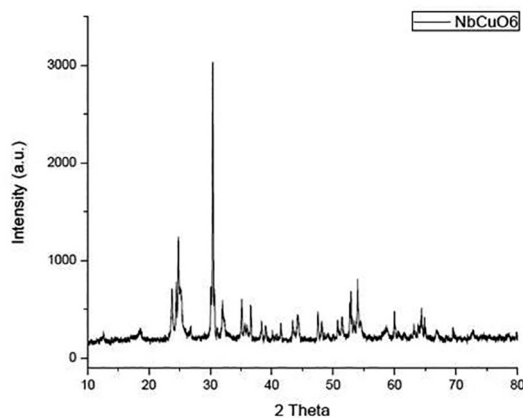


**Figure 5:** XRD pattern for the copper-niobium mixed oxide.

Rietveld's refining method was used to compare the observed XRD pattern with the one obtained from the calculations of the mathematical profile from structural data of the identified phase.

Figure 6 presents the refined XRD pattern, indicating the presence of  $\text{CuNb}_2\text{O}_6$  with orthorhombic structure. It was possible to calculate crystallographic parameters that are presented on Table 2.

### 3.2.2 XRF and EDS

Fluorescence analysis can, when coupled with XRD data, provide bases to evaluate both elemental and phase

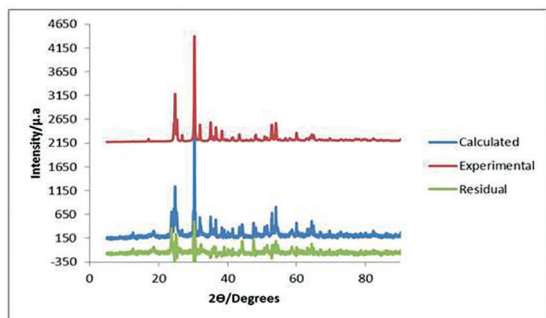


**Figure 6:** XRD spectra refined according to Rietveld method.

**Table 2:** Rietveld refinement of 25%CuNb<sub>2</sub>O<sub>6</sub> using Maud Software.

Phases	a(Å)	b(Å)	c (Å)	α(°)	β(°)	γ (°)
CuNb <sub>2</sub> O <sub>6</sub>	14.06	5.58	5.58	90	90	90
Density (g/cm <sup>3</sup> )	Cell volume (Å <sup>3</sup> )	Crystallite size (nm)	(%) weight	S		
5.71	4.45	384.5	100	1.49		

composition. Table 3 refers to elemental composition found on niobium and copper oxide. XRF data indicates the presence of copper; however, as this analysis is semi-quantitative, differences between expected and observed values can be noted. Also, as copper nitrate is a highly hygroscopic compound, differences on weighted and theoretical values can be attained.

EDS' results are presented on Table 4. Copper was also identified on the produced compound, confirming XRF and XRD data. Obtained values are compatible with those verified by XRF.

### 3.2.3. SEM analysis

Morphological aspects of CuNb<sub>2</sub>O<sub>6</sub> were observed through Scanning Electron Microscopy. Figures 7(a) and (b) present the observed morphology. It can be seen that the compound is highly agglomerated as it is composed of fine particles of different sizes. On Figure 7(b) the presence of randomly dispersed pores can be noted. Those present themselves with different sizes and shapes, which is an expected characteristic of this material.

**Table 3:** XRF elemental analysis of 25%CuNb<sub>2</sub>O<sub>6</sub>.

Analyte	Molar (%)
Nb	76.75
Cu	23.25

**Table 4:** EDS elemental analysis of the 25%CuNb<sub>2</sub>O<sub>6</sub> compound.

Element	(%) Molar
Oxygen	43.42
Copper	22.95
Niobium	33.67

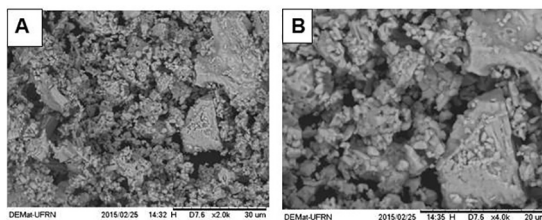


**Figure 7:** SEM images for the copper-niobium mixed oxide, (a) 2000x and (b) 4000x.

In general, CuNb<sub>2</sub>O<sub>6</sub> as obtained in this process, is produced as an agglomerated powder with particles with platelet's morphology with various sizes. According to Fan 1991<sup>16</sup>, this behavior is explained on the basis of Van der Waals' theory, as short distances forces' effect become more pronounced for materials with nanoscale sizes. Toniolo, 2004<sup>17</sup> explains this phenomenon on the basis of the minimization of free energy, as coalesced nuclei provide fewer interfaces with the medium.

## 4. Conclusions

The studied synthesis' method has proved to be effective for the production of the niobium precursor [tris oxalate monohydrate ammonium oxiniobate] which, as TG/DTA analysis showed, decomposes into NH<sub>3</sub>, CO, CO<sub>2</sub> and H<sub>2</sub>O to form niobium oxide with the temperature increase. The physical mixture of this precursor with copper nitrate followed by calcination produced niobium and copper mixed oxide.

XRD spectra of the precursor confirmed the amorphous characteristic of it. Morphological observations revealed the presence of agglomerated particles with platelets' shape.

The doping process was considered feasible for the production of mixed copper-niobium oxide, as XRD analysis indicated the formation of single phase CuNb<sub>2</sub>O<sub>6</sub>. EDS and XRF evaluation also showed the presence of copper in the calcining product in composition close to theoretical values. Rietveld's refinement of the microstructure was performed and attained a small deviation coefficient, which indicates the consistency of the produced crystallographic information with the material and identified phase.

The mixed oxide compound's morphology is basically an agglomerated powder of different size and forms, some in the shape of platelets and some with spherical appearance. These differing morphologies are attributed to the attraction and coalescence of nuclei/small particles.

## 5. Acknowledgments

Programa de Pós-Graduação em Ciências e Engenharia de Materiais- PPGCEM;

Universidade Federal do Rio Grande do Norte- UFRN; Laboratório de Materiais Cerâmicos e Metais Especiais – LMCME;

Laboratório de Materiais Nanoestruturados e Reatores Catalíticos – LAMNRC;



Coordenação de Aperfeiçoamento de Pessoal de Nível Superior-CAPES

## 6. References

1. Lima, J. M. G.; *Relatório Técnico 20 – Perfil da Mineração do Nióbio*, Ministério de Minas e Energia, 2010.
2. European Commission. *Critical raw materials for the EU*. [cited 2015 Apr 25]. Available from: [http://ec.europa.eu/growth/sectors/raw-materials/specific-interest/critical/index\\_en.htm](http://ec.europa.eu/growth/sectors/raw-materials/specific-interest/critical/index_en.htm)
3. Lopes OF, Mendonça VR, Silva FBF, Paris EC, Ribeiro C. Óxidos de nióbio: uma visão sobre a síntese do  $\text{Nb}_2\text{O}_5$  e sua aplicação em fotocatalise heterogênea. *Química Nova*. 2015;38(1):106-117.
4. Leite RCC, Comim A, Leme CR, Pereira ES, Queiroz R. *Nióbio: Uma Conquista Nacional*. São Paulo: Livraria Duas Cidades; 1988.
5. Tanabe K. Application of niobium oxides as catalysts. *Catalysis Today*. 1990;8(1):1-11.
6. Ziolk M. Niobium-containing catalysts—the state of the art. *Catalysis Today*. 2003;78(1-4):47-64.
7. Oliveira LCA, Gonçalves M, Oliveira DQL, Guarieiro, ALN, Pereira MC. Synthesis and catalytic properties on oxidation reaction of goethite containing niobium. *Química Nova*. 2007;30(4):925-929.
8. Cardoso FP, Nogueira AE, Patrício PSO, Oliveira LCA. Effect of tungsten doping on catalytic properties of niobium oxide. *Journal of the Brazilian Chemical Society*. 2012;23(4):702-709.
9. Lee JD. *Química Inorgânica: não tão concisa*. Tradução da 5ª edição inglesa. São Paulo: Edgard Blucher; 1999.
10. Marthner RW, Weiss R, Rohmer R. The crystal structures of ammonium oxotrioxalatonibate monohydrate and ammonium diperoxodioxalatonibate monohydrate. *Journal of the Chemical Society D: Chemical Communications*. 1969;2:70-71.
11. Medeiros FFP. *Síntese de carbeto de tungstênio e nióbio a baixa temperatura, através de reação gás-sólido em reator de leito fixo* [Tese de doutorado]. Natal: Centro de Tecnologia, Departamento de Engenharia Química, Programa de Pós-Graduação em Engenharia Química, Universidade Federal do Rio Grande do Norte; 2002. 145p.
12. Oliveira SA. *Avaliação cinética e potencial do  $\text{Nb}_2\text{O}_5$  obtido a partir de um complexo de nióbio para formação do oleato de metila através da reação de esterificação do ácido oleico* [Dissertação de Mestrado]. Natal: Programa de Pós-Graduação em Engenharia Química, Área de Concentração: Engenharia de Processos – Universidade Federal do Rio Grande do Norte; 2014.
13. Vasconcelos BR, Morais AMV, Lopes FWB, Souza CP. Estudo da variação da concentração de cu na/no  $\text{CuNb}_2\text{O}_6$  sintetizado a partir de reação sólido-sólido. In: *Anais XVIII Congresso Brasileiro de Engenharia Química COBEQ*; 2010 Set 19-22; Foz do Iguaçu, PR.
14. Marta L, Zaharescu M, Macarovici C. Thermal and structural investigation of some oxalato-niobium complexes I potassium tris(oxalato)oxiniobate. *Revue Roumaine de Chimie*. 1979;24:1115-1122.
15. Lu L, Sahajwalla V, Kong C, Harris D. Quantitative X-ray diffraction analysis and its application to various coals. *Carbon*. 2001;39(12):1821-1833.
16. Fan M. Ceramic and glasses. In: *Engineered Materials Handbook*, v. 4. Materials Park: ASM International; 1991. p.270.
17. Toniolo JC. *Síntese de Pós de Alumina Nanocristalina por Combustão em solução* [Dissertação de Mestrado]. Porto Alegre: Programa de Pós-Graduação em Engenharia de Minas, Metalúrgica e de Materiais. Escola de Engenharia. Universidade Federal do Rio Grande do Sul; 2004.